JOURNAL OF MATERIALS SCIENCE: MATERIALS IN MEDICINE **11** (2000) 11–17

Needle-like apatite-leucite glass-ceramic as a base material for the veneering of metal restorations in dentistry

W. HÖLAND, V. RHEINBERGER, S. WEGNER, M. FRANK
Ivoclar Ltd., FL-9494 Schaan, Principality of Liechtenstein

A needle-like apatite-leucite glass-ceramic was prepared in the SiO_2-Al_2O_3-Na_2O-K_2O-P_2O_5-F system. Nucleation and crystallization processes were studied in bulk and powdered samples. The crystallization of leucite follows the mechanism of surface crystallization. After the precipitation of $NaCaPO_4$ crystals and another unknown crystal phase, the formation of needle-like apatite is based on a volume nucleation and crystallization process. The mechanism of the formation of needle-like apatite differs to those of apatite precipitation in glass-ceramics. The morphology of needle-like apatite is comparable to that of apatite in natural teeth.

The properties of the glass-ceramic, especially the good chemical durability, the optical properties, as well as mechanical and thermal properties allow glass-ceramic to be used as a main component in a bio-material for the veneering of metal restorations in dentistry.

1. Introduction

In restorative dentistry the materials used to veneer the metal frameworks of crowns, bridges, or inlays are predominantly ceramics containing leucite. These ceramics are sintered products made of K_2O-rich feldspar and various other components. When these base materials are heat treated, a crystal phase of the leucite type, $KAlSi_2O_6$, is formed by uncontrolled crystallization. These crystals are embedded in a glass matrix. They are responsible for the favorable coefficient of thermal expansion of approximately 12 to $14 \times 10^{-6} K^{-1}$ m/m of the veneering ceramic. This high coefficient of thermal expansion matches that of metal frameworks for dental restorations [1].

A needle-like apatite-leucite glass-ceramic [2, 3] in the form of a sintered material has been developed to provide a real glass-ceramic for the veneering of metal restorations for the first time ever.

This article presents the mechanisms of controlled crystallization applied in the production of apatite-leucite glass-ceramics in contrast to those of the uncontrolled crystallization of leucite ceramics. The formation of the microstructure is examined in particular. In this context, the formation of needle-like apatite is also addressed. An important regulation variable in the crystallization of needle-like crystals is nucleation. This mechanism is studied on the basis of initial results for the nucleation of needle-like apatite in glass-ceramics [4].

Since it had been difficult to recognize all the working principles involved in the formation of glass-ceramics of the apatite-leucite type, an international team of researchers (TC7 / Technical Committee 7) of ICG (International Commission on Glass) was appointed to study this subject in 1995. The initial results of their investigations are cited in this article.

Other significant properties of glass-ceramics are also presented in the results regarding controlled crystallization.

It is interesting to note that needle-like apatite, which is one of the main components of natural teeth, had previously been unknown in glass-ceramics. Nevesely [5], Jaha *et al.* [6] and Yubao *et al.* [7] however, have been able to synthesize apatite demonstrating this morphology in inorganic monolithic reactions.

In recent articles, a mullite glass-ceramic with needle-like apatite has also been presented (Hill and Wood [8]), apart from the apatite-leucite glass-ceramic.

Furthermore, the difference between bioactive dental products and dental glass-ceramics is also addressed. While apatite glass-ceramics of the apatite-wollastonite type according to Kokubo [9] demonstrate a high surface reactivity, these properties are undesirable in glass-ceramics for restorative dental applications.

2. Experimental

A special composition was selected to study the nucleation and crystallization processes of apatite-leucite glass-ceramics in the composition range of these materials [2]: 49–58 wt % SiO_2, 11–19 Al_2O_3, 9–23 K_2O, 1–10 Na_2O, 2–12 CaO, 0.5–6 P_2O_5, 1–9 ZrO_2, 0.2–2.5 F and additives up to 6 wt %. This composition was also examined by the international team of researchers mentioned:

54.8 wt % SiO_2, 14.1 Al_2O_3, 8.4 Na_2O, 10.6 K_2O, 4.9 CaO, 1.0 ZrO_2, 0.3 TiO_2, 3.9 P_2O_5, 0.8 CeO_2, 0.2 Li_2O, 0.3 B_2O_3 and 0.7 F.

A glass of this composition was melted at approximately 1500 °C. Once the liquid glass melt had been homogenized, two different types of base glasses were produced: (A) monolithic glass block, (B) glass powder.

The glass block measured approximately 1 × 2 × 10 cm and the glass powder demonstrated a particle size of less than 90 µm. Both types of base glasses underwent subsequent heat treatment in the temperature range of 700 to 1050 °C. Nucleation and crystallization took place in this range. Therefore, in-situ crystallization occurred, i.e. crystallization by the exposure to heat, without the addition of foreign substances.

Following the selective heat treatment in the nucleation range (up to 700 °C) and in the crystallization range (preferably 950 and 1050 °C), the microstructure was examined with a scanning electron microscope/SEM (LEO, D, Type DSM 962) and for the nature teeth investigation a high resolution SEM (LEO, D, Type 982 Gemini). In addition to the investigation of the microstructure, an analysis of the reactions in the nucleation and crystallization range was conducted using differential scanning calometry (Netzsch, D, Type 404).

Parallel to the SEM analysis of the microstructure, a qualitative and partially quantitative determination of the crystal phase was conducted by X-ray diffraction analysis/XRD (Siemens, D, Type D 5005).

The following properties are of particular interest in regard to the application of the glass-ceramic as a restorative material in dentistry: chemical durability in hot 4% acetic acid, translucency, bending strength. The determination of these properties was conducted according to specific dental standards [10]. The chemical durability were established according to ISO test standards [10] by immersing the materials in acetic acid for 16 h at 80 °C. The limit for layering restorative materials is a maximum of 100 µg/cm^2.

3. Results and discussion

3.1. Crystallization of monolithic glass

The glass block was cut into smaller monolithic bodies (dimensions of approximately 5 × 5 × 5 mm), the nucleation and crystallization behavior of which was studied. The findings served as models for the glass powder.

An analysis of the crystallization processes in the range of 900 to 1050 °C clearly demonstrated that leucite crystals grow inwards from the sample surface, according to the mechanism of surface crystallization. This behavior is distinct in Fig. 1. The special growth mechanism of leucite resembles that of leucite in the CaO and P_2O_5-free SiO_2-Al_2O_3-K_2O glass-ceramic system determined by Höland *et al.* [11].

In contrast to monolithic samples, the surface crystallization of leucite can be initiated and controlled in the glass powder. It is possible, therefore, to produce a specific amount of leucite in the glass-ceramic as described at a later stage in this article (section 3.2).

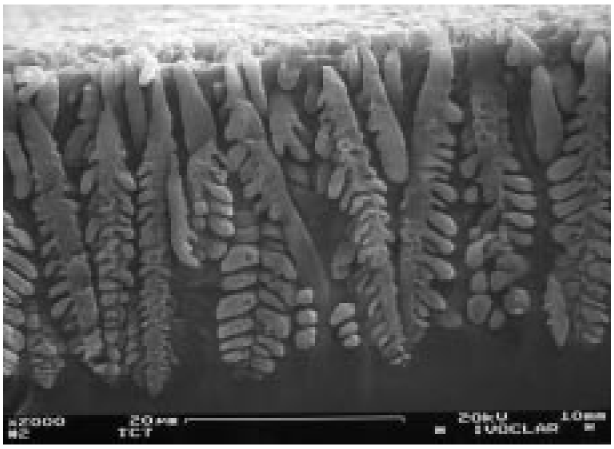

Figure 1 Crystallization of leucite in a monolithic glass after heat treatment at 900 °C/1 h. The leucite grows from the surface towards the center of the sample. SEM (etching 10 s, 3% HF).

In comparison to leucite formation, the crystallization of apatite in the monolithic glass as well as in the glass powder proceeds according to a different mechanism: volume crystallization. Controlled volume crystallization is initiated by controlled nucleation. Fig. 2 shows that nucleation takes place according to liquid-liquid phase separation of the base glass. In this figure, two glass phases are discernible: a glass matrix and a droplet-shaped glass phase.

The DSC examinations revealed an interesting phenomenon: The glass demonstrates two endothermic reactions (Fig. 3). In earlier investigations [4], these two endothermic reactions were described as two transformation ranges of two glassy phases, a silica rich glassy matrix phase and a glass droplet phase rich in CaO and P_2O_5. However, the results of the present study showed that the endothermic reaction at lower temperatures (565 °C) corresponds to the Tg-range of the glassy matrix. But the second reaction (634 °C), which appeared as a reversible peak, was a result of a transformation of a crystal phase. The first range appears as an excursion of the zero line of the DSC curve, which is typical of a transformation of the first order. The second peak, which is unusual for a transformation of the first order, indicates polymorphic transformation of a crystalline phase. XRD structural investigations conducted on samples following heat treatment before (550 and 610 °C) and after (700 °C) this peak characterized this crystalline phase as an

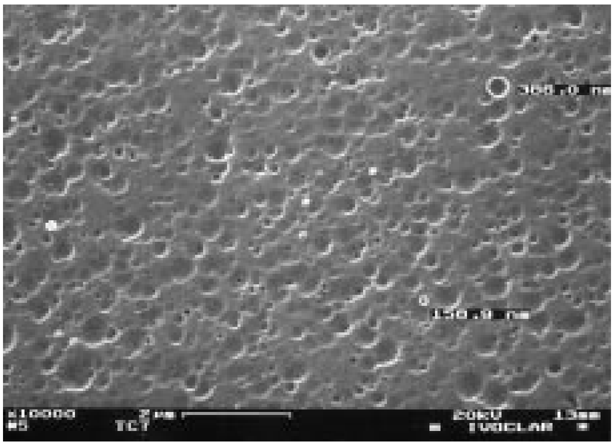

Figure 2 Microstructure of the base glass characterized by liquid-liquid phase separation. SEM (etching 10 s, 3% HF).

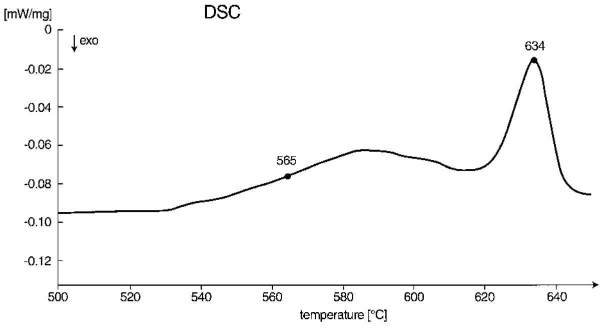

Figure 3 DSC function of the base glass.

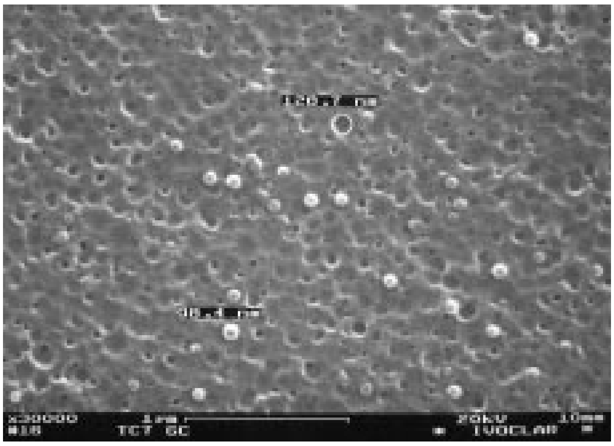

Figure 5 Primary crystal formation in apatite-leucite glass-ceramics. Crystals of $NaCaPO_4$ precipitate as very tiny species at 580 °C after 15 min. SEM (10 s, 2.5% HF).

orthophosphate of $NaCaPO_4$ [12]. This crystal phase is characterized to show polymorphic transformation from low- to high form at approx. 650 °C.

The X-ray diffraction pattern of $NaCaPO_4$ crystals in the glass-ceramic is shown in Fig. 4a) in comparison to other crystal phases of the glass-ceramic. The lattice of $NaCaPO_4$ is orthorhombic corresponding to the Space Group Pnam. The lattice constants are $a = 6.797\mathring{A}$, $b = 9.165\mathring{A}$ and $c = 5.406\mathring{A}$ on the basis of the ICDD (International Center of Diffraction Data) pattern 29-1193.

This very interesting result demonstrated the primary crystal formation in apatite-leucite glass-ceramics as the precipitation of $NaCaPO_4$ in a temperature range of 550 to 610 °C. Fig. 5 shows a typical microstructure of the primary crystal formation as very tiny species. When this microstructure is investigated in detail it is not obvious if all glassy droplet phases of the base glass (Fig. 2) were transferred to crystal phases. Thus, it might also be possible that the interface energy between glassy droplet and glassy matrix play an important role in the nucleation process. On the other hand, it is important to note that the crystal formation of $NaCaPO_4$ was not characterized by an exothermic reaction of the DSC investigation.

The following solid state reaction in the process of glass-ceramic formation was investigated at temperatures above 610 °C. Here, a new interesting phenomenon was discovered. XRD investigations showed the precipitation of an additional crystalline phase at 640 °C and no $NaCaPO_4$ crystal were present any longer. Thus, $NaCaPO_4$ crystals dissolved and a new crystal phase formed. But the XRD diagram (Fig. 4b) could not interpreted on the basis of ICDD (International Center of Diffraction Data). Therefore, this crystal phase was called ''X-crystal phase''.

Also the crystallization of apatite was observed after the precipitation of the X-phase at a heat treatment at 700 °C for 8 h. A typical microstructure of the primary formation of apatite is shown in Fig. 6. In this figure, it is interesting to note that a high density of fluoroapatite and X-phase crystals is reached, with the maximum diameter of the crystallites measuring approx. 100 nm. Thus, at this stage the primary fluoroapatite, $Ca_{10}(PO_4)_6F_2$, does not show a needle-like habit.

However, if the sample heat treated at 700 °C for 8 h (Fig. 6) is subsequently heat treated at 1050 °C for 2 h, needle-like apatite formed. These needle-like crystals are shown in the microstructure of Fig. 7. The XRD pattern (Fig. 4c) of this sample (microstructure of Fig. 7) showed fluoroapatite and the X-crystal phase. The lattice of fluoroapatite is hexagonal corresponding to Space Group P63/m. The lattice constants are $a = b = 9.36840\mathring{A}$, $c = 6.88410\mathring{A}$, $\alpha = \beta = 90\,°C$, $\gamma = 120\,°C$ on the basis to the ICDD-pattern 15-876. When the microstructure of the glass-ceramic that was formed at 700 and 1050 °C is investigated, it is surprising that some amorphous droplet

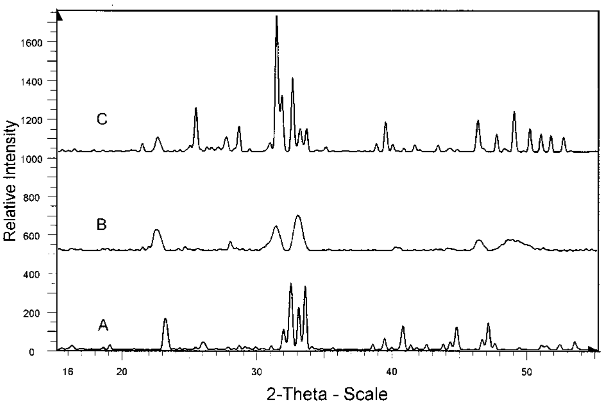

Figure 4 X-ray diffraction pattern of the base glass for apatite-leucite glass-ceramic after treatment at a) 580 °C, 15 min; b) 640 °C, 15 min; c) 700 °C, 8 h and 1050 °C, 2 h. a) represents $NaCaPO_4$ crystals, b) X-crystal phase and c) X-crystal phase and fluoroapatite.

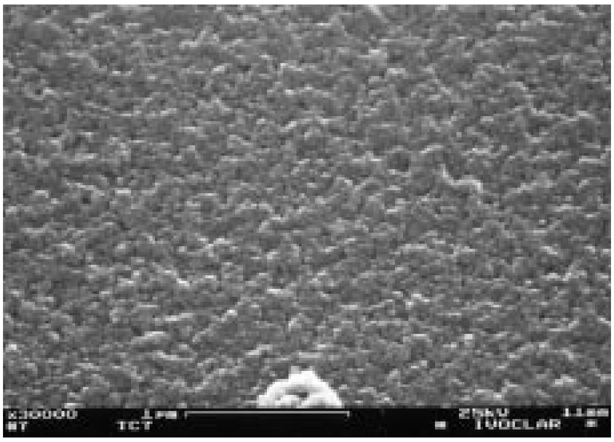

Figure 6 Fluoroapatite and X-crystal formation at 700 °C/8 h. SEM (10 s, 2.5% HF).

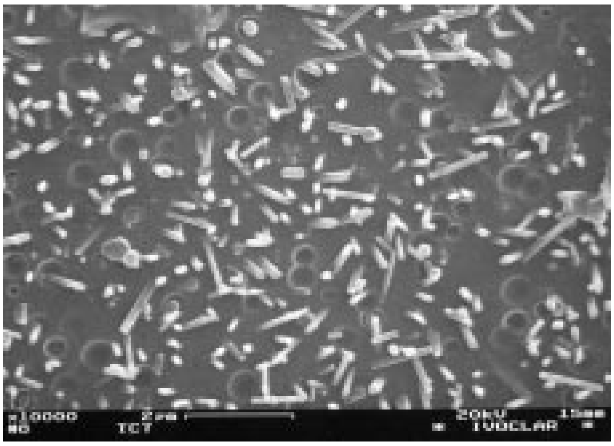

Figure 7 Crystallization of needle-like apatite in the volume of the glass-ceramic after heat treatment at 700 °C/8 h and additionally at 1050 °C/2 h. SEM (10 s, 2.5% HF).

phases were either not transformed into crystals or were rebuilt from other phases as a result of a solid state reaction.

The net result of all solid state phase formations in apatite-leucite glass-ceramics from room temperature up to 1050 °C are shown in the scheme of Table I. Based on this results, it must be mentioned that the formation of needle-like apatite in glass-ceramics differs to the formation of apatite in other glass-ceramics, e.g. apatite–wollastonite glass-ceramics (Kokubo [9]) or mica-apatite glass-ceramics (Höland *et al.* [13, 14]). Apatite formation in mica glass-ceramics was a result of a homogeneous crystallization of a $CaO\text{-}P_2O_5$ rich glassy droplet phase. But needle-like apatite formation is a result of a series of solid state reactions prior to apatite formation.

The investigation of the overall nucleation and crystallization of apatite is important for the processing of needle-like apatite in a large scale technical production. Therefore, the nucleation of apatite was studied by Schmidhauser [15] and demonstrated by means of nucleation/crystallization curves. Fig. 8 shows the course of these curves in the nucleation of apatite. The smallest spherical cyrstallites visible with the scanning electron microscope were counted by surface and represented as a function of the heat treatment (nucleation time and nucleation temperature). These values were recorded (Fig. 8). Subsequently, the values with the same nucleus densities (determined as the number of nuclei per surface) were connected by a curve. In this way, curves representing the nucleus density of 10, 20, 30, 40, 50 and 60 particles / $10^{-6}m^2$ were formed. The evaluation of this nucleation/crystallization function demonstrated a TTT (time-temperature-transformation) functions according to the theory of Uhlmann [16]. The minimum of this function establishes the optimal nucleation temperature. According to the results shown in Fig. 8, the optimal nucleation temperature for needle-like apatite in apatite-leucite glass-ceramics is between 700 and 750 °C. This result corresponds to the apatite formation demonstrated in Table I.

3.2. Crystallization of glass powder (sintered glass-ceramics)

The two partial processes, that is, the growth of leucite and that of apatite, were specifically influenced at the same time by the controlled crystallization of glass powder.

Fig. 9 shows that leucite and apatite crystals are

TABLE I Crystal formation in the volume* of apatite-leucite glass ceramics

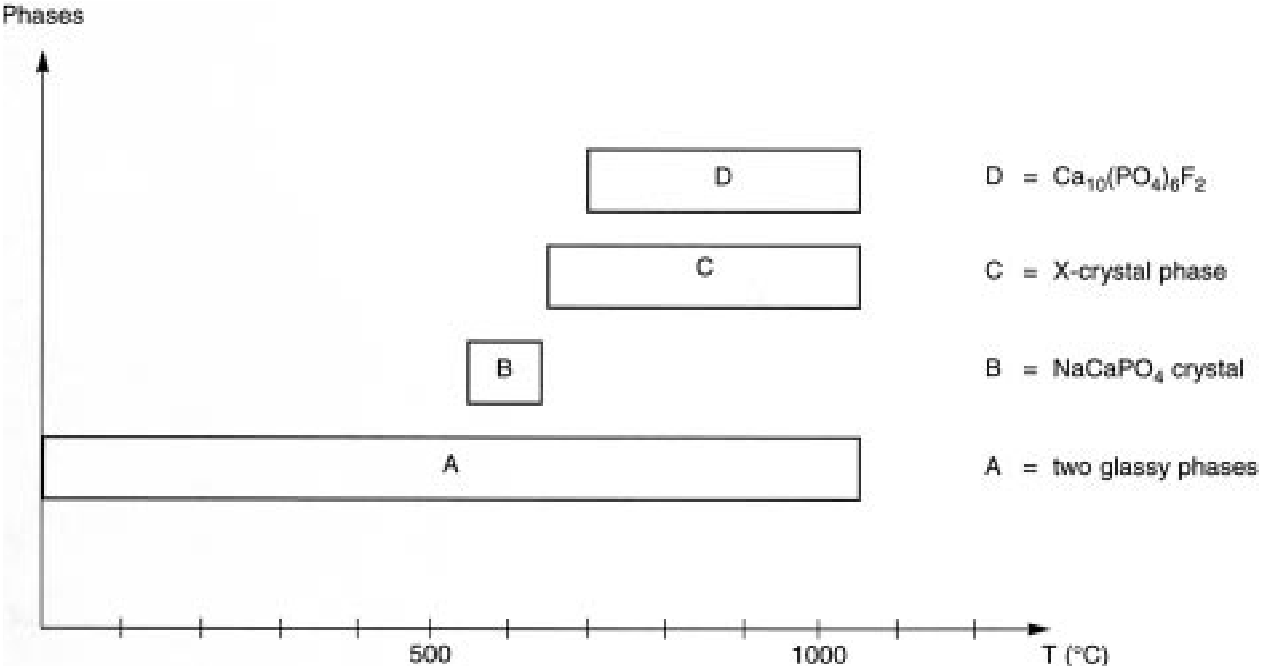

---

* It must be mentioned that leucite is precipitated on the basis of a surface crystallization mechanism. End temperature of investigation: 1050 °C.

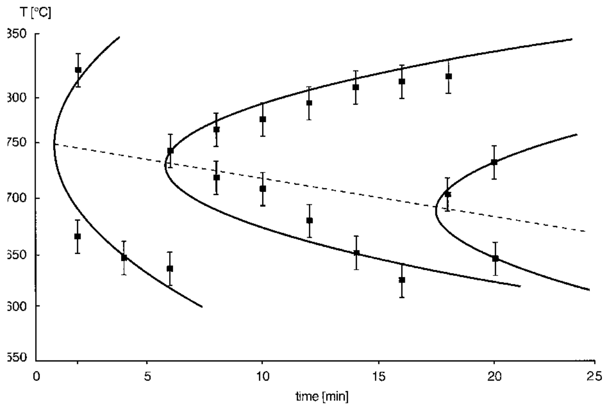

Figure 8 Nucleation/crystallization diagram of apatite in the base glass for apatite-leucite glass-ceramic. The marked points indicate the number of primary apatite crystals per area (number / 10^{-6} m^2).

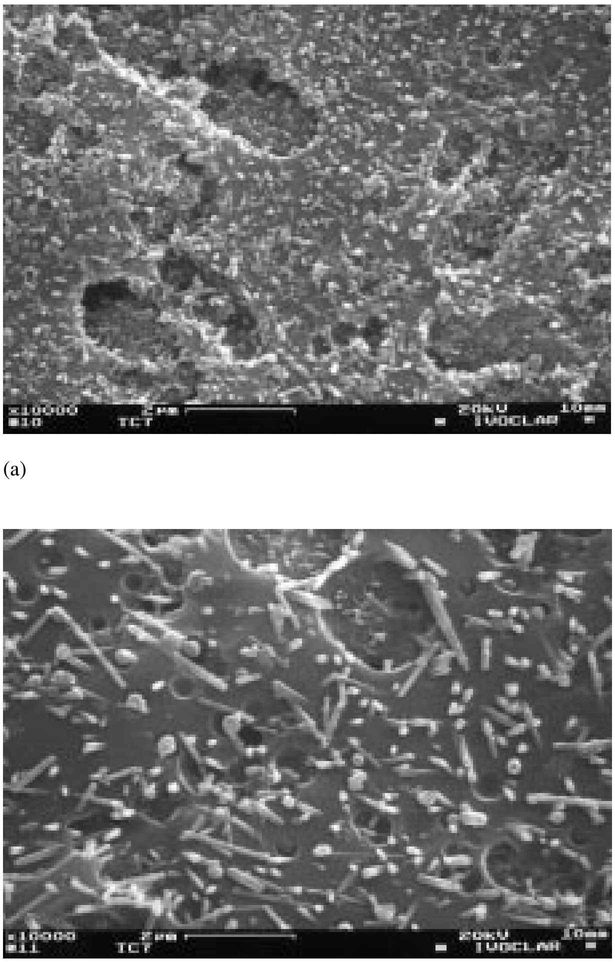

(a)

(b)

Figure 9 Microstructure of apatite-leucite glass-ceramic for dental restorations. Heat treatment of the glass powder at 850 °C /1 h (Fig. 9a) and 1050 °C/1 h (Fig. 9b). The apatite crystals measure approx. 0.1–0.5 (Fig. 9a) and 1–2 µm (Fig. 9b) in diameter. The leucite crystals measure approx 2 µm. SEM (etching 10 s, 3% HF).

formed in glass powders after heat treatment at 850 °C for 1 h (Fig. 9a) or at 1050 °C for 1 h (Fig. 9b). The leucite crystals measure approximately 1 to 2 µm in diameter. The considerably smaller needle-like apatite crystals are located between the leucite crystals with regard to the morphology of these apatite crystals, it should be mentioned that the needle-like apatite formed in the glass-ceramic is comparable to the needle-like apatite in natural teeth. For comparison, a special high resolution SEM micrograph was carried out to investigate the needle-like apatite of a tooth in the area of dental enamel. The result of this investigation is shown in Fig. 10. The needle-like apatite in natural teeth measures of approx. 200–500 nm in diameter.

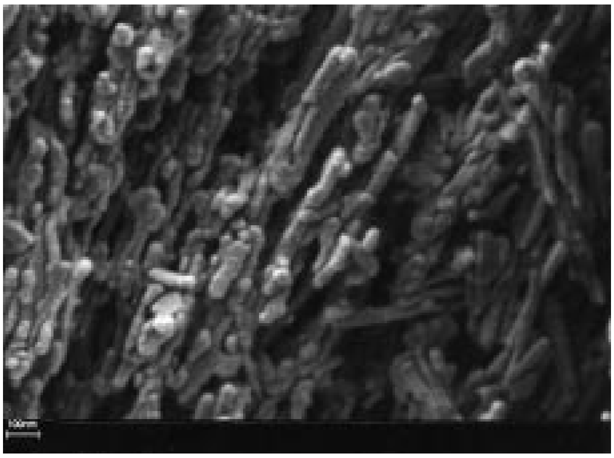

Figure 10 High resolution SEM of natural tooth (etching 30 s, 1 n HCl).

The apatite growth process in apatite-leucite glass-ceramic demonstrates an additional peculiarity. As assumed in the initial investigations (Höland [17]) and subsequently confirmed by Müller *et al.* [18] in the course of research done for the above TC 7, the crystals grow according to the principle of Ostwald ripening. Thus, it was established that the number of crystals decreases, while the length of the crystals increases at 1050 °C, the longer the heat treatment lasts (see Fig. 11). A similar functional relationship occurred with regard to the diameter of the crystallites. The total volume of the apatite crystals in the glass-ceramic, however, remained constant. These findings established all the criteria for Ostwald ripening, the process in which large crystals grow at the expense of smaller ones.

Relative to the volume percent of the crystal phases, 5–10 vol% apatite and 10–25 vol% leucite is typical for this type of glass-ceramic. As a result of the variation of the crystalline content, it is also possible to control the properties of the glass-ceramic, e.g. the optical properties, the mechanical properties such as abrasion and stability, and the thermal properties such as the coefficient of thermal expansion of glass-ceramics. The

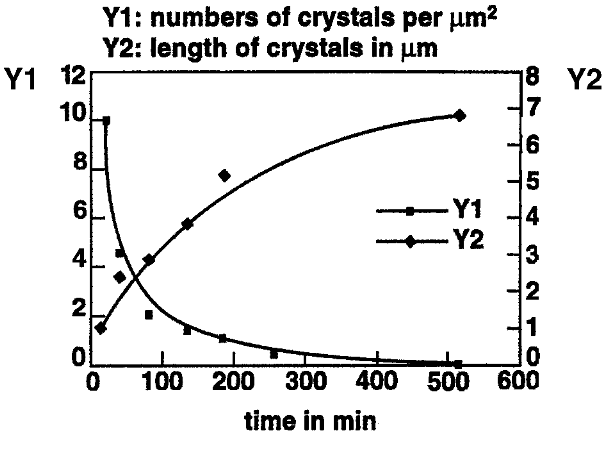

Figure 11 Number and length of needle-like apatite as a function of time for apatite-leucite glass-ceramic at 1050 °C.

following results will show that the properties can be controlled by controlling the microstructure. Two examples of glass-ceramics, namely a glass-ceramic formed at 850 °C (microstructure see Fig. 9a) and 1050 °C (microstructure see Fig. 9b) will be discussed. The results are shown in Table II. For example, a coefficient of thermal expansion of $14.1 \times 10^{-6}\,K^{-1}$ m/m, translucency of 5.8% (acc. to [19]), and bending strength (acc. to [10]) of 106 MPa has been established for a glass-ceramic formed at 1050 °C with the microstructure shown in Fig. 9b. The speciality of the microstructure of the glass-ceramic of Fig. 9b is its crystal length of apatite of approx. 1–2 μm. If the crystals of apatite are smaller than 1 μm (Fig. 9a), a glass-ceramic is generated having a higher translucency than the previous one. This precisely means in detail, that the translucency can be increased from 5.8% to 10.4% (Table II). These values clearly show that the translucency can be adjusted to match that of natural teeth.

The optical properties of glass-ceramics and also abrasion are favorably influenced by fluoroapatite crystals. *In vitro* investigations of a glass-ceramic composite, which contained apatite-leucite glass-ceramic showed the lowest abrasion in comparison to other leucite glass-ceramics. Fig. 12 shows these results of investigations after different masticatory cycles. Also, the antagonist tooth showed the lowest abrasion [20].

The chemical durability of the glass-ceramic is very good. The loss of mass of the above glass-ceramic in acidic acid was less than 80 μg/cm². These results correspond to Szabo *et al.* [21] in the course of research done for the above TC 7.

TABLE II Properties of sintered glass-ceramic of needle-like apatite-leucite

Processing and properties	Type 1	Type 2
heat treatment of glass granules	850 °C/1 h	1050 °C/1 h
translucency (acc. to [19])	10.4%	5.8%
glass phase transformation point	510 °C	520 °C
linear thermal expansion coefficient (100–400 °C)	$14.8 \cdot 10^{-6}\,K^{-1}$m/m	$14.1 \cdot 10^{-6}\,K^{-1}$ m/m
chemical durability (acc. to [10])	60 μg/(cm²)	70 μg/(cm²)
bonding strength (acc. to [10])	100 ± 22 MPa	106 ± 21 MPa

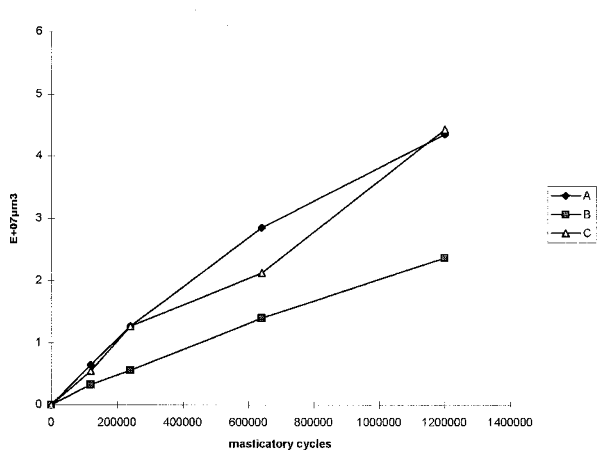

Figure 12 Abrasion of apatite-leucite glass-ceramic (B) in comparison to leucite ceramics (A, C). Antagonist: natural tooth.

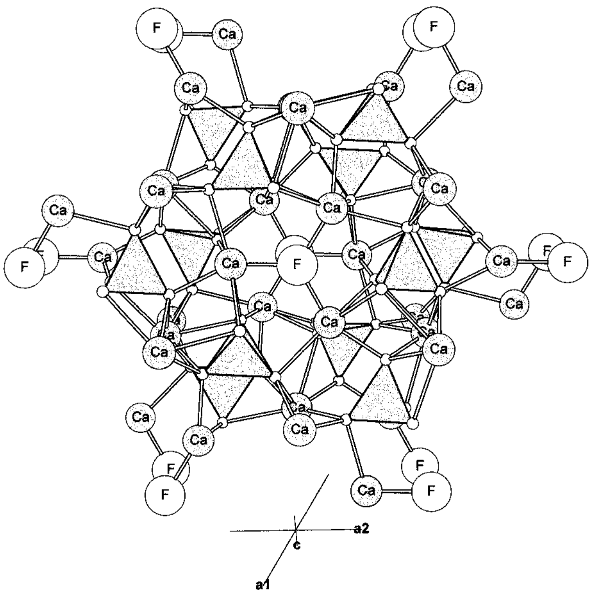

Figure 13 Crystal structure of fluoroapatite. The excerpt from the structure shows the location of the F-ions in particular. Determined according to [23].

The glass and crystal phases are responsible for this particularly favorable chemical durability of the glass-ceramic. The fluoroapatite precipitated in the glass-ceramic shows that fluoroapatite is more chemically durable than hydroxyl apatite or carbonato apatite found in natural bone (Le Geros [22]). Since bioactivity is undesirable in this biomaterial, the high chemical durability of fluoroapatite is very favorable for applications in restorative dentistry. The crystal structure of fluorapatite is shown in Fig. 13. The structure was tipped slightly to make the position of the F-ions more visible. It must be noted that the size of the ions has been somewhat adjusted to make them more easily discernible.

4. Conclusion

The development of new materials has reached a stage, where it has become possible to produce a biomaterial that contains similar building blocks, in the form of needle-like apatite, to those of living teeth. The needle-like apatite favorably influences the optical properties and various mechanical parameters of the material. The fluorine content and the chemically durable glass matrix further enhance the chemical properties of the material.

These characteristics of needle-like apatite-leucite glass-ceramic meet the standards for dental application. In fact, the material can be used as a main component in a bio-material for coating a large variety of dental alloys.

References

1. W. J. O'BRIAN, Dental porcelains. In: ''An outline of dental materials and their selection''. edited by W.J. O'Brian and G. Ryge, (WB Saunders Comp., Philadelphia, 1978) 180–194.
2. W. HÖLAND, M. FRANK, M. SCHWEIGER and V. RHEINBERGER, *Glastech. Ber. Glass Sci. Technol.* **67C** (1994) 117–122.

3. W. HÖLAND, V. RHEINBERGER, M. FRANK and M. SCHWEIGER, *Bioceramics* **8** Pergamon, Oxford (1995) 299–301.
4. W. HÖLAND, V. RHEINBERGER and M. FRANK, Proceedings ICG Congress 1998, San Francisco, *J. Non-Cryst. Sol.* (submitted for publication).
5. H. NEWESELY, Mechanism and action of trace elements in the mineralization of dental hard tissue, Zyma SA (1972).
6. L. J. JAHA, S. M. BEST, J. C. KNOWLES, I. REHMAN, J. D. SANTOS and W. BONFIELD, *J. Mat. Sci.; Mat. in Med.* **8** (1997) 185–191.
7. U. YUBAO, K. DE GROOT, J. DE WIJN, C. P. A. T. KLEIN and S. V. D. MEER, *ibid.* **5** (1994) 326–331.
8. R. HILL and W. WOOD, *ibid.* **6** (1995) 311–318.
9. T. KOKUBO, *Bol. Soc. Esp. Ceram.* **VID 31-C** (1992) 1: 119–138.
10. International Standard ISO 6872, Dental Ceramic, Genf ISO, (1984).
11. W. HÖLAND, M. FRANK and V. RHEINBERGER, *J. Non. Cryst. Sol.* **180** (1995) 292–307.
12. M. BEN AMARA, M. V. LASSE, G. LE FLEM and D. HAGENMULLER, *Acta Cryst.* **39 C** (1983) 1483–1485.
13. W. HÖLAND, W. GÖTZ, G. CARL and W. VOGEL, *Cells and Mater.* **2** (1992) 105–112.
14. W. HÖLAND, *J. Non-Cryst. Sol* **219** (1997) 192–197.
15. B. SCHMIDHAUSER, Diploma degree, ETH Zürich (1997).
16. D. R. UHLMANN, In: W.D. Kingery/H.K. Bowen and D.R. Uhlmann. ‘‘Introduction to ceramics’’. (John Wiley & Sons, New York, 1976) 347–348.
17. W. HÖLAND, *Phosphorus Res. Bull* **6** (1996) 111–114.
18. R. MÜLLER, L. A. ABU-HILAL, S. REINSCH and W. HÖLAND, *J. Mat. Sci.* **34** (1999) 65–69.
19. British standard, BS 5612, Dental Porcelain (1978).
20. R. MÜSSNER, Ivoclar Ltd. internal report (1997).
21. I. SZABO, B. NAGY, G. VÖLKSCH and W. HÖLAND, *J. Non-Cryst. Sol* (to be published).
22. R. Z. LE GEROS and J. P. LE GEROS, In ‘‘An introduction to bioceramics’’, L.L. Hench and J. Wilson, edited by (World Scientific, Singapore, 1993) 139–180.
23. A. T. SÄNGER and W. F. KUHS, *Z. Krist.* **199** (1992) 123–148.

Received 24 August
and accepted 24 December 1998